ELSEVIER

Journal of Molecular Catalysis A: Chemical 179 (2002) 93–100

JOURNAL OF MOLECULAR CATALYSIS A: CHEMICAL

www.elsevier.com/locate/molcata

Multidentate phosphanes as ligands in rhodium catalyzed hydroformylation of 1-hexene

Pekka Suomalainen [a], Riitta Laitinen [b], Sirpa Jääskeläinen [a], Matti Haukka [a], Jouni T. Pursiainen [b], Tapani A. Pakkanen [a,*]

[a] *Department of Chemistry, University of Joensuu, P.O. Box 111, FIN-80101 Joensuu, Finland*
[b] *Department of Chemistry, University of Oulu, P.O. Box 3000, FIN-90401 Oulu, Finland*

Received 31 May 2001; accepted 14 September 2001

Abstract

Triphenylphosphine derivatives modified with thiomethyl (SCH_3) and methoxy (OCH_3) groups in *ortho*- and *para*-position of the phenyl ring(s) were screened in situ $Rh_4(CO)_{12}$ catalyzed 1-hexene hydroformylation reaction. The effect of amount and position of the substituents on the hydroformylation results are discussed in terms of geometric and electronic properties of the ligands. The ab initio molecular modeling methods were used to calculate the ground state structures of the free ligands and their higher energy conformers. Cone angle calculations were used to evaluate the steric attributes of the calculated ligand structures. Additionally, study was made of the reactions between the methoxy substituted phosphanes and $Rh_2(\mu\text{-}Cl)_2(CO)_4$. The crystal structure of *trans*-$Rh(CO)Cl(o\text{-}OOP)_2$ (**1**) is reported.

Keywords: 1-Hexene hydroformylation reaction; Catalytic behavior; Ligand structure

1. Introduction

Bi- and multidentate phosphorus ligands with electronically different substituents, capable of behaving either as chelating or as open-chain ligands, are well documented in the context of homogeneous transition metal catalyzed reactions. It has been proposed that, during the catalytic cycle, the substrate can replace the more weakly coordinated donor site, and thus, accelerate the catalytic reactions.

Perhaps the most widely studied donor combinations are various P–O ligands, as reviewed extensively by Bader and Lindner [1]. Mixed P–S ligands are less studied, although good results have been achieved in carbonylation [2], hydroformylation [3], and asymmetric catalysis [4].

The current paper is a continuation to our earlier studies on *ortho*-substituted triphenylphosphane derivatives: (*o*-thiomethylphenyl)diphenylphosphane, (*o*-methoxyphenyl)diphenylphosphane, and (*o*-*N*,*N*′-dimethylaminophenyl)diphenyl-phosphine [5,6]. Here, we focus on the corresponding multidentate triphenylphosphane ligands having methoxy and thiomethyl groups in *ortho*- and *para*-positions of the phenyl rings.

Through systematic variation in amount, position, and type of the substituent groups in the ligand, we hoped to be able to find structure, activity and structure, regioselectivity trends.

To assist in this, ab initio Hartree–Fock calculations were performed to obtain the free ligand geometries. In addition, to incorporate the flexibility and steric

* Corresponding author. Tel.: +358-13-2513345; fax: +358-13-2513344.
E-mail address: tapani.pakkanen@joenssu.fi (T.A. Pakkanen).

1381-1169/02/$ – see front matter
PII: S1381-1169(01)00400-9

requirements of the ligands, conformational analysis and cone angle [7] measurements were carried out. Furthermore, coordination properties for possibly hemilabile methoxy-substituted phosphanes were investigated in reaction with $Rh_2(\mu\text{-}Cl)_2(CO)_4$.

2. Results and discussion

2.1. Ligands

The methoxy and thiomethyl substituted phosphanes used in this study are listed in Table 1. Extending our previous studies [5,8], we investigated several multidentate phosphane ligands by molecular modeling. Geometry optimizations and conformational analyses were calculated at Hartree–Fock level using the 3-21G* basis set. To classify the ligands by steric character, cone angle measurements were done for all conformers.

Table 2 presents the calculated cone angles for energy minimized structures as well as for higher energy conformers within 100 kJ/mol of the global minimum. Cone angles varied widely, from 152° for *p*-SP to 262° for *o*-SSSP, with steric crowding greatest for

Table 1
Structures and abbreviations for ligands

Abbreviation	Structure (HF/3-21G*)	Abbreviation	Structure (HF/3-21G*)
o-SP (*o*-thiomethylphenyl)-diphenylphosphine [18]	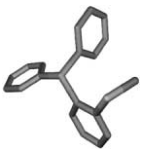	*p*-S–*o*-OOP (*p*-thiomethylphenyl)-bis(*o*-methoxyphenyl)phosphine [19]	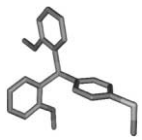
o-SSP bis(o-thiomethylphenyl)-phenylphosphine [18]	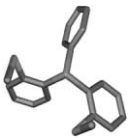	*p*-O–*o*-OOP (*p*-methoxyphenyl)-bis(*o*-methoxyphenyl)phosphine [19]	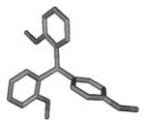
o-SSSP tris(*o*-thiomethylphenyl)-phosphine [18]	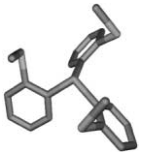	*p*-O–*o*-SSP (*p*-methoxyphenyl)-bis(*o*-thiomethylphenyl)phosphine [19]	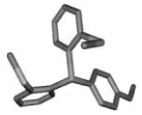
p-SP (*p*-thiomethylphenyl)-diphenylphosphine [18]	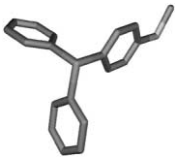	*o*-OOSP (*o*-thiomethylphenyl)-bis(*o*-methoxyphenyl)phosphine [20]	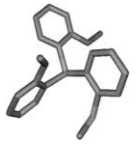
o-OP (*o*-methoxyphenyl)-diphenylphosphine [18]	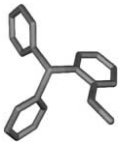	*p*-S–*o*-SSP (*p*-thiomethylphenyl)-bis(*o*-thiomethylphenyl)phosphine [19]	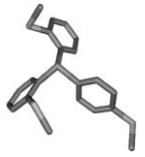
o-OOP bis(*o*-methoxyphenyl)-phosphine [18]	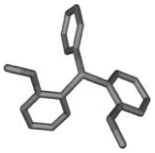	*o*-OOOP tris(*o*-methoxyphenyl)-phosphine [18]	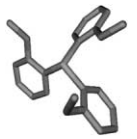

Table 2
Steric requirements of ligands

Ligand	Θ (degree)	Flexibility range
o-SP	158	153–158
o-SSP	223	166–223
o-SSSP	262	167–262
o-OP	166	153–166
o-OOP	183	165–183
o-OOOP	205	169–205
p-SP	152	–
p-S–*o*-SSP	196	–
p-O–*o*-OOP	185	–
p-S–*o*-OOP	186	–
p-O–*o*-SSP	198	–

the ground state "strain-free" conformers. However, those conformers are unlikely to be present when the ligand is coordinated to metal, particularly in the case of bulky ligands. Scheme 1 shows the conformational variation for the *o*-SSSP ligand. As moving to higher energy the phenyl rings begins to rotate, the substituent groups fold inside the cone, thus, no longer determining the maximum cone angle. This behavior was similar for all the ligands.

2.2. Synthesis and characterization of rhodium phosphine complexes

Equimolar amounts of $Rh_2(\mu\text{-}Cl)_2(CO)_4$ and *o*-OOP ligand reacted in methanol solution through the chloride bridge splitting route to yield a yellow precipitate, which was characterized crystallographically as *trans*-Rh(CO)Cl(*o*-OOP)$_2$ (**1**) (Fig. 1).

The analogous *trans*-Rh(CO)Cl(*o*-OP)$_2$ structure was recently reported by us [5]. The IR spectrum of **1** shows a CO stretching vibration at 1968 cm^{-1}, while the ^{31}P-NMR spectrum gives a doublet at 20.5 ppm with J_{Rh-P} of 137 Hz. The reaction proceeded similarly at lower ligand to rhodium ratio (L/Rh = 1/2), but resulted in IR absorption at higher wave number,

	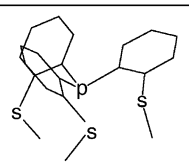	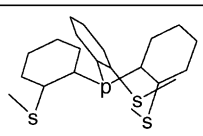	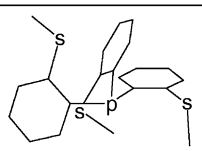	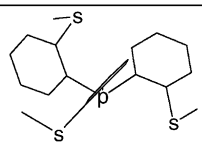
ΔE (kJ / mol)	Global minimum	19.8	35.5	40.4
Θ (deg)	262	180	227	173
	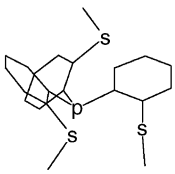	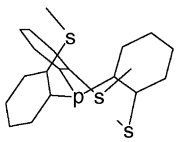	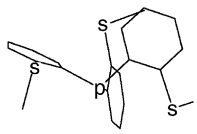	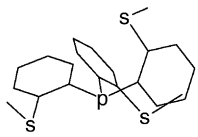
ΔE (kJ / mol)	42.1	44.9	66.3	69.2
Θ (deg)	227	171	167	173

Scheme 1. Low lying conformations of *o*-SSSP ligand.

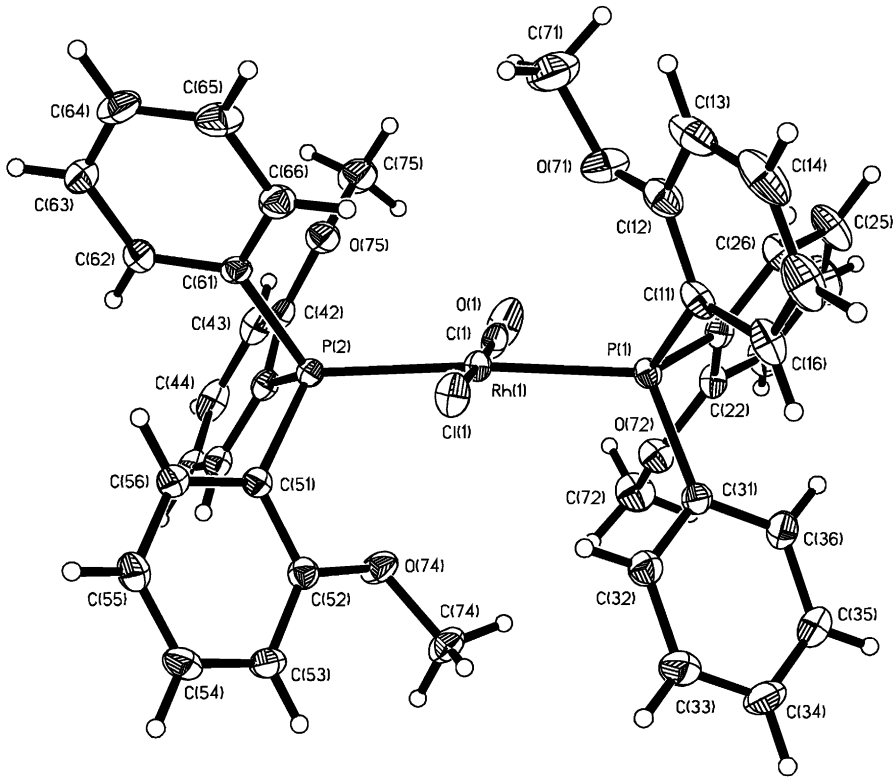

Fig. 1. Ortep drawing of *trans*-Rh(CO)Cl(*o*-OOP)2 with thermal ellipsoids at 50% level.

at 1999 cm^{-1}, representative of Rh(CO)Cl(*o*-OOP) (**2**) compound, with the ligand chelating via oxygen and phosphorus.

Similarly, the reaction between $Rh_2(\mu\text{-}Cl)_2(CO)_4$ and *o*-OOOP (L/Rh = 1/2) resulted in the chelate structure *trans*-Rh(CO)Cl(*o*-OOOP) (**3**). Both the CO stretching vibration in IR at 1995 cm^{-1} and the doublet in ^{31}P-NMR at 38.2 ppm (165Hz) are indicative of such species. The elemental analysis of compounds **2** and **3** are consisted with the chelating species as well.

2.3. Catalysis

Studies of closely related phosphane ligands revealed distinct correlations between the catalytic behavior and structure of the ligands. Results of the 1-hexene hydroformylation experiments are shown in Tables 3 and 4.

At L/Rh ratio of 10 (Table 3), the conversion and the total aldehyde selectivity dropped rapidly with the degree of substitution of the ligand; thus, no activity was observed with the *o*-SSP and *o*-SSSP ligands. Likewise, regioselectivity was affected by the size of the ligand; the normal to branched ratio (n:i) increased linearly as a function of the cone angle. However, enhanced n:i ratios compared to PPh_3 could also be due to the greater basicity of the ligands [9,10].

In view of the low hydroformylation activity as well as the high isomerization activity with the *o*-thioanisyl ligands, the ligand to rhodium ratio was lowered. At L/Rh ratio of 2, the conversion levels were roughly the same with the different catalyst systems, but again crowding of the *ortho*-position of the ligand had a negative effect on the total aldehyde selectivity. Further, the effect was more pronounced with methoxy derivatives (decrease in conversion from 54 to 37% going from *o*-SP to *o*-SSSP and from 49 to 26% going from *o*-OP to *o*-OOOP) (Fig. 2). Cone angle measurements of the free ligands showed the thiomethyl substituted ligands to be sterically more demanding, which would

Table 3
1-Hexene hydroformylation results (L/Rh = 10)[a]

Ligand	θ	Conversion	*S* (hexane)	*S* (isomers)	*S* (2-Ep)	*S* (2-Mh)	*S* (h)	*S* (ald)	n/i
–	–	86	0	80	2	8	11	20	1.1
PPh_3	149	88	0	81	2	7	10	19	1.2
o-SP	158	88	0	81	1	7	11	19	1.4
o-OP	166	86	0	86	1	5	9	14	1.7
o-OOP	183	30	2	87	0	3	8	10	2.7
o-OOOP	205	17	3	86	0	3	8	10	2.8
o-SSP	223	0	0	0	0	0	0	0	–
o-SSSP	262	0	0	0	0	0	0	0	–

[a] 15 bar (CO/H_2=1); 80 °C; 6 h; 1-hexene, 15.5 mmol; toluene, 5 ml; $Rh_4(CO)_{12}$, 1.9×10^{-2} mmol; L/Rh = 10 *S* (isomers): total amount of 2- and 3-hexenes; *S* (2-Ep): selectivity to 2-ethylpentanal; *S* (2-Mh): selectivity to 2-methylhexanal; *S* (h): selectivity to 1-heptanal; *S* (ald): total aldehyde selectivity.

suggest the reverse order in selectivities. However, in our recent studies we found the *o*-SP ligand to behave as chelating ligand, even under severe reaction conditions, whereas the analogous methoxy ligand (*o*-OP) was observed to bind solely monodentately through the phosphorus atom. Although, here we were able to show bidentate coordination mode with methoxy ligands (*o*-OOP and *o*-OOOP), we presume that the chelate ring is too labile to be present in catalytic environment. Thus, we conclude that the difference in selectivity can be explained in terms of the different binding modes of the methoxy and thiomethyl substituted phosphanes.

When the substituent group thiomethyl or methoxy was moved from *ortho*- to *para*-position the selectivity to aldehydes was improved from 37 to 45% going from *o*-SSSP to *p*-S–*o*-SSP and from 26 to 40% going from *o*-OOOP to *p*-O–*o*-OOP. Decreased steric crowding in the vicinity of the phosphorus made the rhodium center more accessible and active for hydroformylation.

However, moving the thiomethyl group from the *o*-SP ligand to *para* position caused the total aldehyde selectivity to drop dramatically, from 54 to 19%. A similar observation was made earlier when CF_3 modified phosphanes were used as ligands in 1-hexene

Table 4
1-Hexene hydroformylation results (L/Rh = 2)[a]

Ligand	Conversion	*S* (isomers)	*S* (2-Ep)	*S* (3-Eh)	*S* (h)	*S* (ald)	n/i
–	95	56	6	19	19	44	0.8
PPh_3	94	58	6	18	18	42	0.8
o-OP	94	51	7	21	22	49	0.8
o-OOP	95	66	5	14	15	34	0.8
o-OOOP	93	74	2	10	14	26	1.1
o-SP	96	46	7	23	24	54	0.8
o-SSP	95	54	7	20	19	46	0.7
o-SSSP	94	63	5	16	17	37	0.8
p-SP	91	81	2	7	10	19	1.1
p-S–*o*-SSP	100	55	6	19	19	45	0.8
p-S–*o*-OOP	100	62	5	16	18	38	0.9
o-OSSP	94	61	5	17	17	39	0.8
p-O–*o*-OOP	95	60	5	16	19	40	0.9
p-O–*o*-SSP	100	57	6	18	19	43	0.8

[a] 20 bar (CO/H_2 = 1); 100 °C; 4 h; 1-hexene, 15.5 mmol; toluene, 5 ml; $Rh_4(CO)_{12}$, 1.9×10^{-2} mmol; L/Rh = 2 *S* (isomers): total amount of 2- and 3-hexenes; *S* (2-Ep): selectivity to 2-ethylpentanal; *S* (3-Mh): selectivity to 3-methylhexanal; *S* (h): selectivity to 1-heptanal; *S* (ald): total aldehyde selectivity.

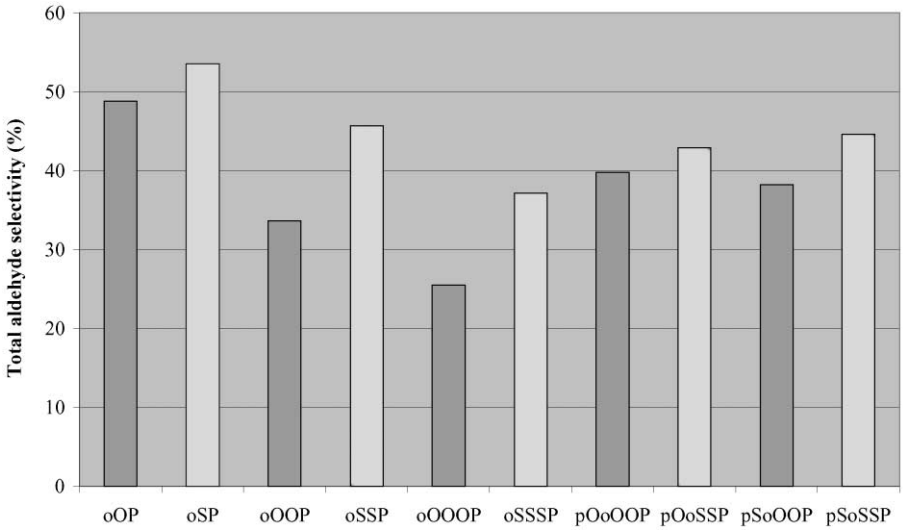

Fig. 2. The aldehyde selectivity of triphenylphosphane ligands modified with thiomethyl and methoxy groups.

hydroformylation [6]. It was proposed there, that the lack of rhodium hydride formation may have affected the reactivity.

3. Experimental part

3.1. Computational details

Gaussian'94 [11] and Sybyl [12] programs were used in modeling. The equilibrium geometries of the ligands were first determined by optimizing the structures by ab initio Hartree–Fock method using a 3-21G* basis set. Starting from the initial geometries, conformational analysis was carried out by rotating the torsional angles of the three phenyl rings. The unsubstituted phenyl ring(s) was rotated 180°, while the substituted phenyl ring(s) was rotated 360° by increments of 20°, resulting in up to ∼6000 different conformers. Based on contour maps of the potential energy surface of the resulting conformers, 20–40 local minima were identified and subsequently optimized by the HF/3-21G* method. The energies of the minima in relation to the ground state are presented in Scheme 1. For cone angle determinations the metal (dummy)–phosphorus distance of 2.28 Å and the van der Waals radii of hydrogen of 1.2 Å were used.

3.2. Metal complexes

3.2.1. Trans-Rh(CO)Cl(o-OOP)$_2$ (1)

$Rh_2(CO)_4Cl_2$ (100 mg, 0.257 mmol) and *o*-OOP (170 mg, 0.53 mmol) were dissolved in methanol in separate flasks, and the ligand solution was added drop-wise to the precursor solution. The yellow precipitate that formed was filtered, washed with methanol, and quickly dried under vacuum. Yellow crystals for X-ray studies were crystallized from a CH_2Cl_2/hexane solution. Elemental analysis for **1**, $C_{41}H_{38}P_2O_5ClRh$: calcd. % of C, 60.72; H, 4.72%; found % of C, 60.11; H, 4.65%. IR (CH_2Cl_2): $\upsilon(CO) = 1968\,cm^{-1}$. ^{31}P-NMR: $\delta = 20.5$ ppm, J(Rh–P) = 137 Hz.

3.2.2. Rh(CO)Cl(o-OOP) (2)

$Rh_2(CO)_4Cl_2$ (25 mg, 0.064 mmol) and *o*-OOP (35 mg, 0.109 mmol) elemental analysis for **2**, $C_{21}H_{19}PO_3ClRh$: calcd. % of C, 51.61; H, 3.92%; found % of C, 51.39; H, 3.99%. IR (CH_2Cl_2): $\upsilon(CO) = 1999\,cm^{-1}$.

3.2.3. Rh(CO)Cl(o-OOOP) (3)

$Rh_2(CO)_4Cl_2$ (100 mg, 0.257 mmol) and *o*-OOP (170 mg, 0.53 mmol) were dissolved in methanol in separate flasks. Before being added to the precursor solution, the ligand solution was slightly

warmed (50 °C) to allow total dissolution. The yellow precipitate, which formed after a few hours of mixing, was filtered, washed with methanol, and quickly dried under vacuum. Elemental analysis for **3**, $C_{22}H_{21}PO_4ClRh$: calcd. % of C, 50.94; H, 4.08%; found % of C, 50.65; H, 4.06%. IR (CH_2Cl_2): $\upsilon(CO) = 1994\,cm^{-1}$. ^{31}P-NMR: $\delta = 38.2$ ppm, $J(Rh–P) = 165$ Hz.

3.3. X-ray crystallography

X-ray diffraction data were collected with a Nonius KappaCCD diffractometer using Mo Kα radiation ($\lambda = 0.71073$ Å) and ϕ-scan data collection mode with a Collect [13] collection program. Denzo and Scalepack [14] programs were used for cell refinements and data reduction. Structure was solved by direct methods using the SIR97 program [15] and the WinGX [16] graphical user interface. Structure refinements were carried out with the SHELXL97 [17] program. Hydrogens were constrained to ride on their parent atoms ($C_{arom}–H = 0.95$ Å, $U_{iso} = 1.2C_{eq}$, $C_{CH_2}–H = 0.99$ Å, $U_{iso} = 1.2C_{eq}$, and $C_{CH_3}–H = 0.98$ Å, $U_{iso} = 1.5C_{eq}$). Crystallographic data (excluding structure factors) for the structure reported in this paper have been deposited with the Cambridge Crystallographic Data Centre as supplementary publication no. CCDC 159195. Copies of the data can be obtained free of charge on application to CCDC, 12 Union Road, Cambridge CB2 1EZ, UK (fax: int. code +44-1223-336-033; E-mail: deposit@ccdc.cam.ac.uk).

Crystallographic data are summarized in Table 6 and selected bond lengths and angles are presented in Table 5. The structure of complex **1** is shown in Fig. 1.

Table 5
Selected bond lengths and angles for compound **1**

Atoms	*trans*-Rh(CO)Cl(*o*-OOP)$_2$ (**1**)
	Bond distances (Å)
Rh–C(1)	1.808 (2)
Rh–Cl(1)	2.398 (5)
Rh–P(1)	2.328 (6)
Rh–P(2)	2.326 (6)
C(1)–O(1)	1.146 (3)
P(1)–C(11)	1.829 (2)
P(1)–C(21)	1.825 (2)
P(1)–C(31)	1.835 (2)
C(12)–O(71)	1.362 (3)
O(71)–C(71)	1.428 (3)
C(22)–O(72)	1.365 (3)
O(72)–C(72)	1.434 (3)
P(2)–C(41)	1.829 (2)
P(2)–C(51)	1.834 (2)
P(2)–C(61)	1.832 (2)
C(52)–O(74)	1.371 (3)
O(74)–C(74)	1.427 (3)
C(42)–O(75)	1.368 (3)
O(75)–C(75)	1.428 (3)
	Bond angles (degree)
P(2)–Rh–P(1)	175.17 (2)
C(1)–Rh–P(2)	91.88 (7)
C(1)–Rh–P(1)	90.87 (7)
C(1)–Rh–Cl	177.17 (8)
P(2)–Rh–Cl	88.24 (2)
P(1)–Rh–Cl	89.21 (2)
O(1)–C(1)–Rh(1)	178.7 (2)
C(12)–O(71)–C(71)	118.9 (2)
C(22)–O(72)–C(72)	117.45 (2)
C(52)–O(74)–C(74)	117.91 (2)
C(42)–O(75)–C(75)	117.56 (2)

3.4. Catalysis

1-Hexene hydroformylation reactions were conducted in a 100 ml autoclave (Berghof) with 60 ml Teflon liner. Experiments were carried out in batch mode with rhodium precursor $Rh_4(CO)_{12}$. The reactor was charged under a nitrogen purge with substrate, rhodium catalyst, ligand, and internal standard (cyclohexane). The autoclave was then sealed and pressurized using a 1:1 mixture of H_2 and CO (MG, 99.997%) to 20 bars. The autoclave was heated to 100 °C, and after four or 6 h reaction it was cooled and returned to normal atmospheric pressure. The reproducibility of the system was confirmed by performing the tests twice.

A disposable inner Teflon liner was used to avoid the accumulation of rhodium on the reactor walls. The purity of the system was also checked with blank runs before each experiment. The products were analyzed with a Hewlett-Packard 5890 GC equipped with a capillary column (HP-1, 1.0 μm × 0.32 mm × 60 m) and a flame-ionization detector. Products were quantified by the internal standard method. In addition, the aldehydes that formed were identified by GC-MS analysis.

Table 6
Crystallographic data for compound **1**

Empirical formula	$C_{41}H_{38}P_2O_5ClRh$
molecular weight	811.06
Crystal size (mm)	0.3 × 0.3 × 0.3
Crystalline system	Triclinic
Space group	P-1
a (Å)	10.1423 (2)
b (Å)	12.8966 (4)
c (Å)	16.1360 (6)
λ (Å)	85.196 (10)
β (degree)	79.239 (2)
γ (degree)	71.758 (2)
V (Å3)	1968.56 (10)
Z	2
D_{calc} (g/cm^3)	1.512
μ (mm^{-1})	0.763
T (K)	150 (2)
θ range (degree)	3.02–27.46
Number of collected rflns	16757
Number of unique rflns	8764
Number of params	482
R_1[a]	0.0320
wR_2[a]	0.0470
Largest difference peak and hole, e (Å^{-3})	0.482 and −0566

[a] $I > 2\sigma$.

4. Conclusions

Hydroformylation tests revealed relationships between the catalytic behavior and structure of the ligands.

The conversion and the total aldehyde selectivity decreased as a function of cone angle and degree of substitution of the ligand. As the substituents were then moved from *ortho*- to *para*-position in the ligand, so as to decrease the steric hindrance near phosphorus and rhodium centers, the selectivity to aldehydes increased.

However, steric requirements did not explain the differences in the catalytic behavior of the two donor types. Higher chemoselectivity of the thiomethyl modified ligands is suggested to arise from the bidentate coordination, and thus, from the more accessible metal center. Although Rh(I) complexes containing methoxy substituted ligands bearing chelate P–O ring were also observed, ring formation was not considered to be strong enough to take place under catalytic environment.

Compared with PPh_3 the regioselectivity (n/i) increased with all of the studied ligands. This was due to the greater steric size and to the greater basicity of the ligands.

Regioselectivity was also dependent on binding mode, and thus, n/i ratios were lower with thiomethyl- than methoxy-modified ligands.

References

[1] A. Bader, E. Lindner, Coord. Chem. Rev. 108 (1991) 27.
[2] M.J. Baker, M.F. Giles, A.G. Orpen, M.J. Taylor, R.J. Watt, J. Chem. Soc., Chem. Commun. (1995) 197.
[3] H.K. Reinius, R.H. Laitinen, A.O.I. Krause, J.T. Pursiainen, Catal. Lett. 60 (1999) 65.
[4] O. Pàmies, M. Dièquez, G. Net, A. Ruiz, C. Claver, Organometallics 19 (2000) 1488.
[5] P. Suomalainen, S. Jääskeläinen, M. Haukka, R.H. Laitinen, J. Pursiainen, T.A. Pakkanen, Eur. J. Inorg. Chem. (2000) 2607.
[6] P. Suomalainen, H.K. Reinius, H. Riihimäki, R.H. Laitinen, S. Jääskeläinen, M. Haukka, J.T. Pursiainen, T.A. Pakkanen, A.O.I. Krause, J. Mol. Catal. 169 (2001) 67.
[7] C.A. Tolman, Chem. Rev. 77 (1977) 313.
[8] L. Hirsivaara, L. Guerricabeitia, M. Haukka, P. Suomalainen, R.H. Laitinen, T.A. Pakkanen, J. Pursiainen, Inorg. Chim. Acta 307 (2000) 47.
[9] J.D. Unruh, J.R. Christenson, J. Mol. Catal. 14 (1982) 19.
[10] W.R. Moser, C.J. Papile, D.A. Brannon, R.A. Duwell, S.J. Weininger, J. Mol. Catal. 41 (1987) 271.
[11] M.J. Frisch, G.W. Trucks, H.B. Schlegel, P.M.W. Gill, B.G. Johnson, M.A. Robb, J.R. Cheeseman, T. Keith, G.A. Petersson, J.A. Montgomery, K. Raghavachari, M.A. Al-Lahman, V.G. Zakrzewski, J.V. Ortiz, J.B. Foresman, J. Cioslowski, B.B. Stefanov, A. Nanayakkara, M. Challacombe, C.Y. Peng, P.Y. Ayala, W. Chen, M.W. Wong, J.L. Andres, E.S. Replogle, R. Gomperts, R.L. Martin, D.J. Fox, J.S. Binkley, D.J. Defrees, J. Baker, J.P. Stewart, M. Head-Gordon, C. Gonzales, J.A. Pople, Gaussian Inc., Pittsburgh, PA, 1995.
[12] Sybyl 6.03; Tripos Associates, 1699 S. Hanley Road, Suite 303, St. Louis, MO 63144.
[13] Collect data collection software, Nonius, 1999.
[14] Z. Otwinowski, W. Minor, In: C.W. Carter Jr., R.M. Sweet (Eds.), Methods in Enzymology, Vol. 276, Macromolecular Crystallography, Part A, Academic Press, New York, 1997, pp. 307–326.
[15] A. Altomare, M.C. Burla, M. Camalli, G.L. Cascarano, C. Giacovazzo, A. Guagliardi, A.G.G. Moliterni, G. Polidori, R.J. Spagna, Appl. Cryst. 32 (1999) 115.
[16] L.J. Farrugia, J. Appl. Cryst. 32 (1999) 837.
[17] G.M. Sheldrick, SHELXL97, Program for Crystal Structure Refinement, University of Göttingen, 1997.
[18] D.W. Meck, G. Dyer, M.O. Workman, Inorg. Synth. 16 (1976) 168.
[19] R. Laitinen, H. Riihimäki, M. Haukka, S. Jääskeläinen, T.A. Pakkanen, J. Pursiainen, Eur. J. Inorg. Chem. (1999) 1253.
[20] R.H. Laitinen, V. Heikkinen, M. Haukka, A.M.P. Koskinen, J. Pursiainen, J. Organom. Chem. 598 (2000) 235.